PHYSICAL REVIEW B **86**, 121404(R) (2012)

Temperature evolution of infrared- and Raman-active phonons in graphite

P. Giura,[1] N. Bonini,[2] G. Creff,[3] J. B. Brubach,[3] P. Roy,[3] and M. Lazzeri[1]
[1]*IMPMC, Université Pierre et Marie Curie, CNRS, 4 place Jussieu, 75005 Paris, France*
[2]*Department of Physics, King's College London, London WC2R 2LS, United Kingdom*
[3]*Synchrotron SOLEIL, l'Orme des Merisiers, Saint-Aubin, BP 48, 91192 Gif-sur-Yvette, France*
(Received 9 July 2012; published 20 September 2012)

We perform a comparative experimental and theoretical study of the temperature dependence up to 700 K of the frequency and linewidths of the graphite E_{1u} and E_{2g} optical phonons ($\sim$1590 and 1580 cm^{-1}) by infrared (IR) and Raman spectroscopy. Despite their similar character, the temperature dependence of the two modes is quite different, e.g., the frequency shift of the IR-active E_{1u} mode is almost twice as big as that of the Raman-active E_{2g} mode. *Ab initio* calculations of the anharmonic properties are in remarkable agreement with measurements and explain the observed behavior.

DOI: 10.1103/PhysRevB.86.121404 PACS number(s): 78.30.Na, 63.22.Rc, 63.20.kg, 71.15.Mb

Thermal properties of sp^2 carbon systems such as graphene[1,2] and carbon nanotubes[3,4] have attracted significant attention, both systems being excellent thermal conductors. In these materials, thermal transport is dominated by lattice vibrations (phonons) and transport can be described properly only once the phonon scattering mechanisms are taken into account. Phonon scattering also plays a major role in nonequilibrium phenomena in which nonthermal phonon populations of carbon materials are induced by optical excitation[5,6] or during electronic transport.[7,8] In general, our understanding of thermal properties is heavily based on theoretical modeling,[9–11] and case studies allowing to validate the models are of primary importance.

The frequency and the linewidth of a phonon, as well as its temperature dependence, are measurable quantities which provide key information about the interatomic interactions.[12] Indeed, even in a perfect crystal, the phonon linewidth is not zero and the phonon frequencies depend on temperature because of anharmonic terms in the interatomic potential (phonon-phonon interaction) and, in the same instance, because of nonadiabatic effects (phonon-electron interactions) when the gap is sufficiently small. Raman spectroscopy certainly has a central role in the study of vibrational properties of sp^2 carbon materials. However, this technique probes only a very small portion of the vibrational degrees of freedom and the use of complementary tools is essential to gain further insight. Infrared (IR) spectroscopy is a natural choice and it can also be used to study planar sp^2 systems.[13,14]

The graphene in-plane antiphase movement of the two unit-cell atoms is a Raman-active zero momentum ($\mathbf{q} = \mathbf{0}$) mode with symmetry E_{2g} (Raman G peak). The G frequency depends on the temperature, and the G peak Raman measurement is currently used as a probe of the local temperature in graphene samples.[1,2] In graphite, the E_{2g} mode splits in two modes with symmetry E_{2g} and E_{1u}, depending on the relative motion of the two graphene planes of the graphite unit cell.[15] The E_{2g} one (in-phase vibration of the two planes) is Raman active and is associated with the well known G peak at $\sim$1582 cm^{-1}. The E_{1u} one (antiphase vibration of the two planes) is IR active and has a slightly higher frequency ($\sim$1590 cm^{-1}). The anomalously large IR intensity of this mode has been the topic of a recent work.[14]

Given the similarities between the E_{2g} and E_{1u} vibrations, their properties are expected to be similar. On the contrary, their linewidths are quite different: At room conditions, the full width at half maximum (FWHM) of the Raman mode is $\sim$13 cm^{-1}, while the FWHM of the IR one is $\sim$4 cm^{-1}. Based on calculations[11] these width differences have been related to the different electron-phonon interaction. Moreover, according to Ref. 11, the Raman mode linewidth decreases by increasing the temperature (this behavior is quite unusual), while the IR linewidth is predicted to increase. Above room temperature, measurements of the temperature dependence of the linewidth and frequency shift of the IR mode are needed for a comparison.

In this Rapid Communication, we present the measurement of the linewidth and the line shift of the infrared-active mode at $\sim$1590 cm^{-1} in highly oriented pyrolitic graphite in the temperature range 293–523 K. For a comparison, we also show Raman spectroscopy measurements of the G peak in a similar temperature range. The results are interpreted by means of *ab initio* calculations of the anharmonic properties.

Raman spectra were measured using a Horiba Jobin Yvon T64000 spectrometer equipped with an Ar laser (514.5 nm). The laser was focused on the sample via a Mitutoyo 20$\times$ long distance objective. The incoming power was selected in order to prevent sample damage and ensure a rather high signal-to-noise ratio. The instrumental resolution obtained by measuring the emission spectrum of neon in the E_{2g} phonon frequency region has been found to be 1.6 cm^{-1} (FWHM of a Gaussian profile). Spectra were recorded by spanning the region (1200–1700 cm^{-1}). The sample was mounted inside an in-house made oven composed of a cartridge heater tightly inserted in a cylindrical copper piece with a little squared open cavity for the incoming light. The heater was connected to a power supply equipped with a thermometer allowing to control the temperature of the cartridge heater. The precision was $\pm$0.1 °C.

IR spectra were measured at the AILES infrared beamline[16] of synchrotron SOLEIL (Saint Aubain, France) using a Bruker IFS125 spectrometer working under vacuum. The temperature was set by using a in-house made oven similar to the one used for the Raman experiments. The sample was aligned in reflection geometry, allowing to acquire reflectivity

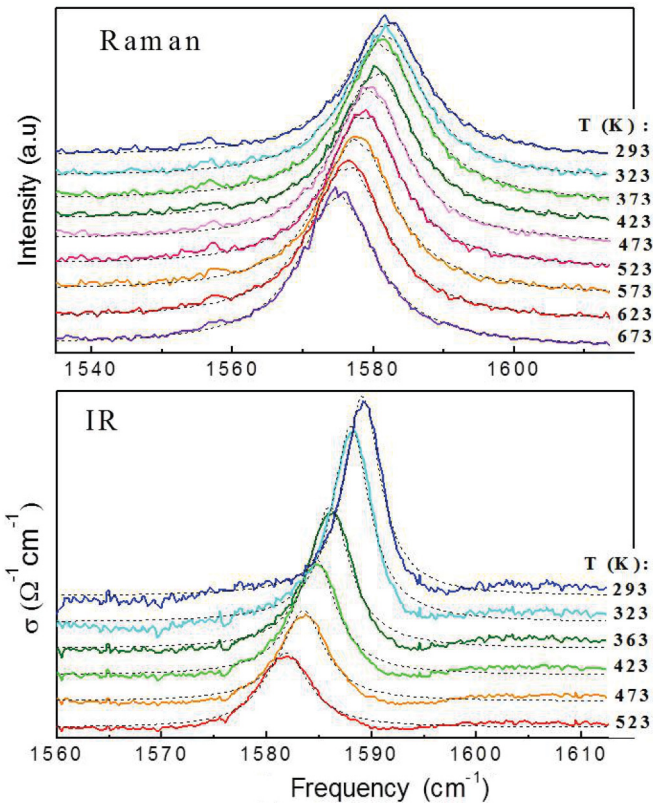

FIG. 1. (Color online) Graphite measured Raman spectra and IR optical conductivity spectra. Spectra taken at different temperatures (T) are vertically shifted for clarity. Each peak is fitted with a single Lorentzian (thin dotted lines).

measurements of the ab-plane transverse excitations at increasing temperatures. The reference was measured at room temperature using a gold mirror mounted in such a way as to replace the sample inside the oven. The entire working setup used was as follows: synchrotron light as the source, KBr as the beam splitter, and mercury cadmium telluride (MCT) as the detector. With this configuration we acquired spectra in the frequency region between 700 and 3500 cm^{-1} with a resolution of 0.1 cm^{-1}. Reflectivity data were treated by a Kramers-Kronig transformation to extract the real part of the optical conductivity $\sigma(\omega)$. The Raman spectra and the conductivity IR spectra, corrected by the respective background, were fitted with a single Lorentzian profile (Fig. 1) to obtain the width and position of the peaks. For a discussion on the asymmetric shape of the IR peak, see Ref. 14.

In a defect-free perfect crystal, phonons have a finite lifetime because they can decay by anharmonic phonon-phonon (ph-ph) scattering or by electron-phonon (e-ph) scattering, this last process being possible in graphite as the electronic gap is zero. The intrinsic linewidth of a phonon can thus be written as a sum of two terms, $\gamma(T) = \gamma^{\text{ph-ph}}(T) + \gamma^{e\text{-ph}}(T)$ (see, e.g., Ref. 11 and references therein), where T is the temperature. The linewidth in a real sample can be larger because of the presence of other scattering mechanisms. Concerning the temperature dependence of the phonon pulsation ω_{ph}, at the lowest order one can distinguish the following contributions:[12]

$$\omega_{\text{ph}} = \omega_0 + \Delta\omega^{le}(T) + \Delta\omega^{3p}(T) + \Delta\omega^{4p}(T) + O(\hbar^2), \quad (1)$$

where ω_0 is the harmonic pulsation at the equilibrium lattice parameters, $\Delta\omega^{le}(T)$ accounts for the variation of the harmonic pulsation by varying the lattice parameters (as a consequence of the thermal expansion), and $\Delta\omega^{3p}(T)$ and $\Delta\omega^{4p}(T)$ can be interpreted as due to anharmonic scattering involving, respectively, three or four phonons (see, e.g., Refs. 12 and 17 and references therein). The three shifts are proportional to $\hbar$ and are thus expected to be of the same order of magnitude. Other terms are $O(\hbar^2)$.

In the present study, we compare the measured linewidths with those calculated in Ref. 11. Reference 11 reports the calculated anharmonic line shift for the Raman mode only. Here, we determine the anharmonic line shift of the IR-active mode using the same approach as Ref. 11. Calculations are performed within density functional theory (plane waves and pseudopotential approach) with the QUANTUM ESPRESSO package.[18] Phonon dispersions are obtained within the linear response approach of Ref. 19. Anharmonic phonon-phonon scattering coefficients are determined by the $2n + 1$ theorem as implemented in Ref. 20. All the computational details have been described in Ref. 11, and, in particular, we use the local density approximation and equilibrium lattice spacing parameters ($a = 2.43$ Å, $c/a = 2.725$).

Figure 2 compares the measured and calculated parameters for the Raman- (E_{2g}) and IR-active (E_{1u}) modes. Measured linewidths are in good agreement with the calculations of

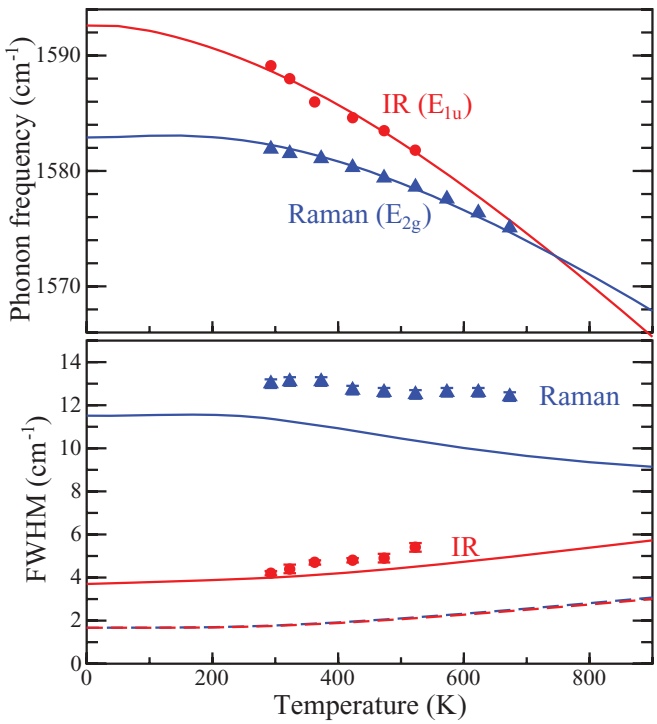

FIG. 2. (Color online) Upper: Graphite phonon frequency as a function of temperature. Symbols are the present measurements from Raman (triangles) and IR (dots). Solid lines are calculations. Lower: Linewidths (full width at half maximum) corresponding to the upper panel measurements. Dashed lines are the contribution to the linewidth due to anharmonic phonon-phonon scattering. Continuous lines are the total intrinsic linewidth (phonon − phonon + electron − phonon; see the text). The calculated Raman shift and the calculated Raman and IR linewidths are taken from Ref. 11.

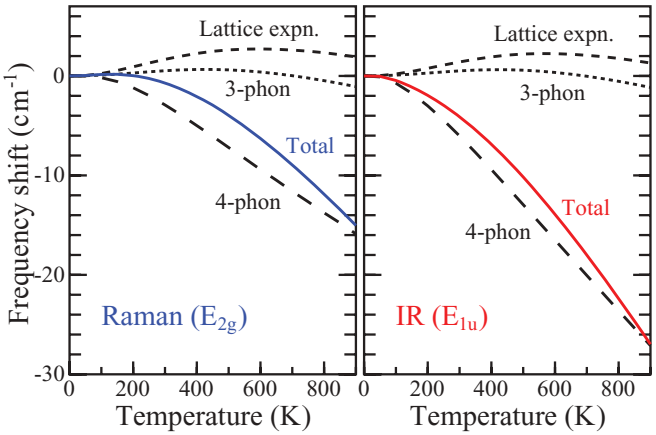

FIG. 3. (Color online) Calculated line shift of the E_{2g} (Raman-active) and E_{1u} (IR-active) $\mathbf{\Gamma}$ phonons of graphite. The total line shift (continuous line) is decomposed into the three-phonon, four-phonon, and lattice expansion contributions. All the contributions are vertically shifted so as to be zero for $T = 0$ K. The $T = 0$ K values are given in the text. Calculations for the Raman mode are taken from Ref. 11.

Ref. 11: The IR linewidth increases when increasing the temperature while the Raman decreases. These trends are directly visible on the raw data of Fig. 1. This behavior was interpreted in Ref. 11 considering the following: (i) The phonon-phonon contribution to the linewidth, $\gamma^{\text{ph-ph}}$, is very similar for the two modes and increases with the temperature (Fig. 1); and (ii) the $\gamma^{e\text{-ph}}$ contribution is significantly more important for the E_{2g} mode and provides the overall temperature decrease of the linewidth.

Figure 2 also shows the line shift. The theoretical curves are vertically shifted to best fit the experimental data, obtaining, for $T = 0$ K, 1592.6 and 1582.9 cm^{-1} for E_{1u} and E_{2g}, respectively. These can be considered as the extrapolated $T = 0$ K experimental frequencies and their difference is 9.7 cm^{-1}. At the equilibrium lattice spacing, the E_{1u} (E_{2g}) frequency is 1614.2 (1604.9) cm^{-1}. To compare with the $T = 0$ K experimental value, one has to add the calculated anharmonic shifts at $T = 0$ K, which are $\Delta\omega^{le}(0) = -17.7$ (-17.7) cm^{-1}, $\Delta\omega^{3p} = -14.2$ (-14.1) cm^{-1}, and $\Delta\omega^{3p} = -1.3$ ($+1.3$) cm^{-1} for the E_{1u} (E_{2g}) mode. The resulting frequency difference is 6.6 cm^{-1}, which underestimates by 3 cm^{-1} the experimental 9.7 cm^{-1} value. By considering frequencies at the generalized gradient approximation (GGA) level,[21] the agreement slightly worsens.

By increasing the temperature from 293 to 523 K, the measured IR frequency shifts by -7.3 cm^{-1}, which is more than twice the corresponding Raman shift, -3.3 cm^{-1}, in agreement with calculations (Fig. 2). To understand this behavior, we decompose the line shift of the two modes into the three T dependent components defined in Eq. (1) (see Fig. 3). The different behavior of the two E_{2g} and E_{1u} modes is almost entirely determined by the corresponding four-phonon scattering terms (Fig. 3).

Why are the four-phonon shifts of the two modes so different? To answer this question, we need to introduce some concepts. Let us consider the interatomic potential energy $\mathcal{E}^{\text{tot}}(\{u_{s\alpha}(\mathbf{R}_l)\})$, where $u_{s\alpha}(\mathbf{R}_l)$ is the displacement from the equilibrium position of the sth atom in the crystal cell identified by the lattice vector $\mathbf{R}_l$ along the α Cartesian coordinate. For a phonon with wave vector $\mathbf{q}$, branch index i, and energy $\hbar\omega_{\mathbf{q}i}$, we define the adimensional phonon displacement as $u_{\mathbf{q}i} = 1/N \sum_{l,s,\alpha} \sqrt{2M_s\omega_{\mathbf{q}i}/\hbar}\, v_{s\alpha}(\mathbf{q}i) u_{s\alpha}(\mathbf{R}_l) e^{-i\mathbf{q}\cdot\mathbf{R}_l}$, $v_{s\alpha}(\mathbf{q}i)$ being the orthogonal phonon eigenmodes normalized on the unit cell, M_s the atomic mass, and N the number of $\mathbf{q}$ points describing the system (or unit cells).

For a phonon $\mathbf{q} = \mathbf{0}$, and branch index i, we define the four-phonon spectral function as

$$S^{4p}_{\mathbf{0}i}(\omega) = \frac{1}{2N\hbar} \sum_{\mathbf{q}j} \frac{\partial^4 \mathcal{E}^{\text{cell}}}{\partial u_{\mathbf{0}i}\, \partial u_{\mathbf{0}i}\, \partial u_{-\mathbf{q}j}\, \partial u_{\mathbf{q}j}} \times (2n_{\mathbf{q}j} + 1)\delta(\omega - \omega_{\mathbf{q}j}), \quad (2)$$

where $\sum_{\boldsymbol{q}}$ is a sum on the Brillouin zone, $\mathcal{E}^{\text{cell}}$ is the unit-cell energy, $n_{\mathbf{q}j}$ is the Bose-statistics occupation of the phonon $(\mathbf{q}j)$, and δ is the Dirac distribution. Equation (2) depends on the temperature only through the terms $n_{\mathbf{q}j}$. The associated four-phonon shift[12,17] can be written as

$$\Delta\omega^{4p}_{\mathbf{0}i} = \int_0^\infty d\omega S^{4p}_{\mathbf{0}i}(\omega).$$

The fourth-order derivatives in Eq. (2) can be interpreted as scattering coefficients among two phonons $\mathbf{0}i$ and the two phonons $-\mathbf{q}j, \mathbf{q}j$. The spectral function separates the contributions from phonons with different energies.

The spectral functions of the two E_{2g} and E_{1u} modes are very similar [Fig. 4(c)], the major differences being near 115 cm^{-1}, where the E_{1u} spectral function shows a peak absent in the E_{2g} one. This peak strongly depends on the temperature (in the temperature range considered) and accounts for the difference in the two E_{2g} and E_{1u} shifts. This peak is associated with the maximum of the graphite phonon density of states (VDOS in Fig. 4) at 115 cm^{-1}, and this maximum is due to the optical out of plane ZO' phonon branch. We remind that, in graphene, the vibration of the atoms perpendicular to the plane is associated with the ZA acoustic branch. In graphite, this branch splits into a branch in which the two graphene planes vibrate in phase, ZA, and a branch in which the two planes vibrate antiphase, ZO' [Figs. 4(a) and 4(b)]. The ZA graphite branch is acoustic, while the ZO' is optical with a 114 cm^{-1} frequency at $\mathbf{q} = \mathbf{0}$. The four-phonon anharmonic coupling [the fourth-order derivative in Eq. (2)] between the E_{1u} mode and the ZO' branch is much stronger than that between the E_{2g} and the ZO'. The presence (absence) of this coupling explains the presence (absence) of the 115 cm^{-1} peak in the spectral decomposition of Fig. 4(c) for the E_{1u} (E_{2g}) mode.

We remark that graphene bilayer also presents an IR-active E_{1u} optical mode and a ZO' mode with a frequency of $\sim$80 cm^{-1},[22] smaller than in graphite. A smaller frequency is associated with a stronger temperature dependence of the ZO' phonon occupation (with respect to the graphite ZO'). This fact suggests that the IR-active E_{1u} mode of the bilayer should present a temperature dependence of the shift stronger than in graphite.

To conclude, we measured the linewidth and frequency shift of the $\mathbf{\Gamma}$ optical phonons E_{1u} (IR active) and E_{2g} (Raman active) of graphite as a function of temperature. Despite

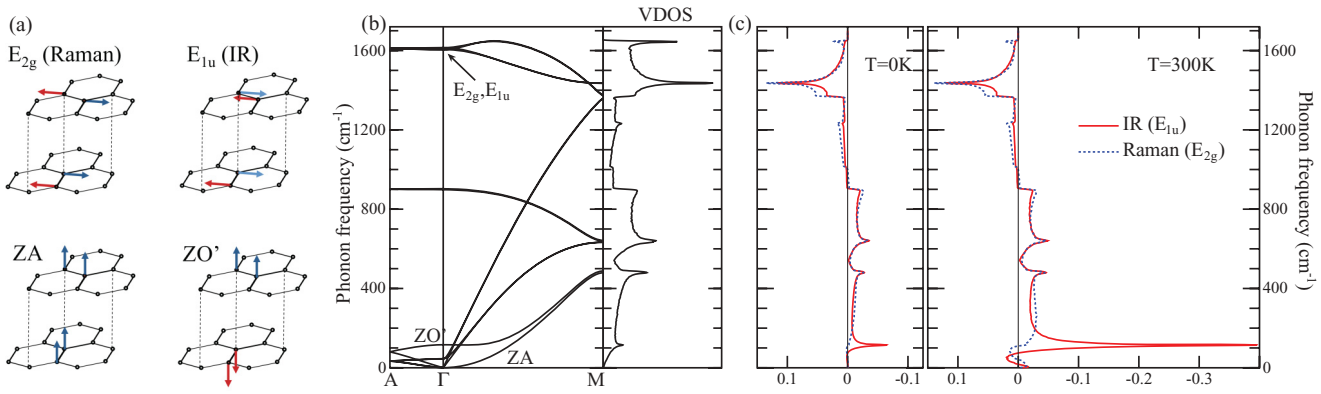

FIG. 4. (Color online) (a) Scheme of various $\mathbf{\Gamma}$ ($\mathbf{q} = \mathbf{0}$) phonons of graphite. (b) Graphite phonon dispersion and related vibrational density of states (VDOS). (c) Spectral decomposition of the four-phonon component of the frequency shift [as defined in Eq. (2)] of the E_{2g} (Raman) and E_{1u}(IR) phonons at temperatures 0 and 300 K.

the similarities between the two E_{1u} and E_{2g} vibrations, their temperature dependence is quite different. The E_{1u} linewidth is almost three times smaller than the E_{2g} one (at room temperature) and, while the E_{1u} linewidth increases by increasing the temperature, the E_{2g} one slightly decreases. Both behaviors are in good agreement with the *ab initio* calculations of Ref. 11. The shifts of the two modes are also very different: By increasing the temperature from 293 to 523 K, the E_{1u} mode shifts by more than twice the corresponding E_{2g} value, in agreement with the present calculations. This difference is explained by the presence (absence) of the four-phonon anharmonic coupling between the E_{1u} (E_{2g}) phonon and the ZO' phonon branch at $\sim$115 cm^{-1}. These findings confirm the accuracy and predictive power of density functional theory calculations in determining anharmonic phonon-phonon scattering in sp^2 carbon systems, a key step in developing realistic models for thermal transport.[9]

Parts of the calculations were done at IDRIS, Project No. 096128.

[1] A. A. Balandin *et al.*, Nano Lett. **8**, 902 (2008).
[2] J. H. Seol *et al.*, Science **328**, 213 (2010).
[3] C. Yu *et al.*, Nano Lett. **5**, 1842 (2005).
[4] E. Pop *et al.*, Nano Lett. **6**, 96 (2006).
[5] I. Chatzakis, H. Yan, D. Song, S. Berciaud, and T. F. Heinz, Phys. Rev. B **83**, 205411 (2011).
[6] M. Scheuch *et al.*, Appl. Phys. Lett. **99**, 211908 (2011).
[7] E. Pop, D. Mann, J. Cao, Q. Wang, K. Goodson, and H. Dai, Phys. Rev. Lett. **95**, 155505 (2005).
[8] M. Lazzeri and F. Mauri, Phys. Rev. B **73**, 165419 (2006).
[9] N. Bonini, J. Garg, and N. Marzari, Nano Lett. **12**, 2673 (2012).
[10] D. L. Nika and A. A. Balandin, J. Phys.: Condens. Matter **24**, 233203 (2012).
[11] N. Bonini, M. Lazzeri, N. Marzari, and F. Mauri, Phys. Rev. Lett. **99**, 176802 (2007).
[12] J. Menendez and M. Cardona, Phys. Rev. B **29**, 2051 (1984).
[13] Z. Q. Li, C. H. Lui, E. Cappelluti, L. Benfatto, K. F. Mak, G. L. Carr, J. Shan, and T. F. Heinz, Phys. Rev. Lett. **108**, 156801 (2012).
[14] M. Manzardo, E. Cappelluti, E. van Heumen, and A. B. Kuzmenko, Phys. Rev. B **86**, 054302 (2012).
[15] F. Tuinstra and J. L. Koenig, J. Chem. Phys. **53**, 1126 (1970); R. J. Nemanich, G. Lucovsky, and S. A. Solin, Solid State Commun. **23**, 117 (1977).
[16] J. B. Brubach *et al.*, in *WIRMS 2009 5th International Workshop on Infrared Microscopy and Spectroscopy with Accelerator Based Sources*, edited by A. Predoi-Cross and B. E. Billinghurst, AIP Conf. Proc., Vol. 1214 (AIP, Melville, NY, 2010), p. 81; P. Roy, M. Rouzieres, Z. M. Qi, and O. Chubar, Infrared Phys. Technol. **49**, 139 (2006).
[17] M. Lazzeri, M. Calandra, and F. Mauri, Phys. Rev. B **68**, 220509(R) (2003).
[18] P. Giannozzi *et al.*, J. Phys.: Condens. Matter **21**, 395502 (2009).
[19] S. Baroni, S. de Gironcoli, A. Dal Corso, and P. Giannozzi, Rev. Mod. Phys. **73**, 515 (2001).
[20] M. Lazzeri and S. de Gironcoli, Phys. Rev. B **65**, 245402 (2002).
[21] N. Mounet and N. Marzari, Phys. Rev. B **71**, 205214 (2005).
[22] C. H. Park, F. Giustino, M. L. Cohen, and S. G. Louie, Nano Lett. **8**, 4229 (2008).